

Cumulant Correlators in 2D and 3D Scale Free Simulations

Dipak Munshi¹ and Adrian L. Melott²

¹ Astronomy Unit, Queen Mary and Westfield College, London E1 4NS, United Kingdom.

² Department of Physics and Astronomy, University of Kansas, Lawrence, Kansas 66045, U.S.A.

Email: D.Munshi@qmw.ac.uk, melott@kusmos.phsx.ukans.edu

Abstract

Shape dependence of higher order correlations introduces complication in direct determination of these quantities. For this reason theoretical and observational progress has been restricted in calculating one point distribution functions and related moments. Methods based on factorial moments of two point count probability distribution (cumulant correlators) were recently shown to be efficient in subtracting discreteness effects and extracting useful information from galaxy catalogs. We use these cumulant correlators Q_{NM} to study clustering in scale free simulations both in two and three dimensions. Using this method in the highly nonlinear regime we were able to separate hierarchal amplitudes Q_3, R_a and R_b associated with different tree graphs contributing to third and fourth order correlation functions. They were found to increase with power on large scales. Results based on factorial moments of one point cumulants show very good agreement with that on cumulant correlators. Comparison of simulation results with perturbation theory and extended perturbation theory were found to be in reasonable agreement. Comparisons were also made against predictions from hierarchal models for higher order correlations. We argue that finite volume corrections are very important for computation of cumulant correlators.

Subject Headings: large scale structure of the universe - galaxies: statistics - methods: data analysis - methods: simulation

1. Introduction

There is growing evidence which suggest that the large scale structure in the universe was formed by the gravitational amplification of small inhomogeneities. Statistical characterization of clustering is important for understanding the dynamics of gravitational clustering. Correlation functions and count in cell statistics are among the oldest and most widely used statistics to quantify clustering. Evaluation of higher order correlation functions with full shape dependence is difficult given limited size of present day galaxy catalogs and numerical simulations (Fry & Peebles 1978, Peebles 1980). Much progress has therefore been made in estimation of volume averages of these quantities (Gaztanaga 1992, Bouchet et al. 1993, Gaztanaga & Frieman 1994, Colombi et al. 1996a, Szapudi et al. 1996), which can be directly related to moments of one point count probability distribution function. Analytical methods based on tree level perturbation theory and loop corrections were used to evaluate these quantities in the quasi-linear regime (Peebles 1980, Juszkiewicz et al. 1993, Bernardeau 1992, Bernardeau 1994, Munshi et al. 1994, Colombi et al. 1992, Scoccimarro & Frieman 1996a-b.). In the highly nonlinear regime, although no full theory exists, scaling models are often used to predict their behaviour (Peebles 1980, Balian & Schaeffer 1989). Computational methods were also developed based on factorial moments to subtract Poisson noise from discrete data. Errors associated with these one point cumulants and other related quantities such as void probability function have also been estimated and correction procedure have been developed (Colombi et al. 1995, Szapudi & Colombi 1996, Munshi et al. 1997).

Although one point quantities carry useful information about dynamics and background geometry averaging associated with such quantities causes a significant loss of information. Alternative methods use correlation of pairs of cells (Szapudi et al. 1992, Meiksin et al. 1992, Szapudi et al. 1995). Cumulant correlators provide a natural generalization of one point cumulants. The hierarchal ansatz in the strong clustering regime and perturbation theory in the weak clustering regime have definite predictions for these quantities. Using cumulant correlators it is possible to separate amplitudes associated with different tree topologies up

to fifth order in the correlation hierarchy. Szapudi & Szalay (1997) have analysed APM data using cumulant correlators. We use these statistics to study scale-free simulations in two and three dimensions (2D and 3D).

In the next section we outline the theoretical framework necessary for using cumulant correlators, predictions from perturbation theory, hierarchal ansatz and extended perturbation theory. In section §3 we describe our numerical simulations and techniques to evaluate cumulant correlators from simulation data. We discuss implications of our results in section §4 and compare it with existing results from galaxy catalogs.

2. Theoretical Predictions

We define factorial moment correlators of a pair of cells of volume l^3 separated by a distance r as

$$w_{kl}(l, r) = \frac{\langle\langle(N_1)_k(N_2)_l\rangle\rangle - \langle(N_1)_k\rangle\langle(N_2)_l\rangle}{\langle N \rangle^{k+l}}; \quad k \neq 0, l \neq 0, \quad (1)$$

and the normalized one point factorial moment

$$w_{k0}(l) = \frac{\langle\langle(N_1)_k\rangle\rangle}{\langle N_1 \rangle^k}, \quad (2)$$

where we have used the notation $(N)_k = N(N-1)\dots(N-k+1)$, and the angular braces $\langle\dots\rangle$ denote average over all possible positions of the cells.

It is possible to relate w_{k0} and w_{kl} to normalized one point cumulants $S_N = \langle\delta^N\rangle/\langle\delta^2\rangle^{(N-1)}$ and cumulant correlators $C_{NM} = \langle\delta^N(\mathbf{x}_1)\delta^M(\mathbf{x}_2)\rangle/\langle\delta(\mathbf{x}_1)\delta(\mathbf{x}_2)\rangle\langle\delta^2\rangle^{(N+M-2)}$. However we find it to easier to work with $Q_N = S_N/N^{(N-2)}$ and $Q_{NM} = C_{NM}/N^{(N-1)}M^{(M-1)}$. While central moments can also be used to computed these quantities, factorial moments are known to be more suitable for subtracting Poisson shot noise.

One can introduce the generating function for the factorial moments in terms of the cumulants Q_N .

$$W(x) = \exp \sum_{N=1}^{\infty} \Gamma_N x^N Q_N \quad (3)$$

where we have defined $\Gamma_N = N^{N-2}\xi_s^{N-1}/N!$ and ξ_s is the volume average of ξ_2 over volume of the cell l^3 .

The generating function can be linked with the one point void probability distribution function. In general Q_N parameters show scale dependence, increasing from quasi-linear phase to highly nonlinear phase. Hierarchal form of correlation functions demand Q_N to be independent of scale in the nonlinear regime.

We can also construct generating function of factorial moments $W(x, y) = \sum_0^{\infty} W_{mn} x^M y^N / m! n!$ which can be related to generating function of cumulant correlators $Q(x, y)$

$$Q(x, y) = \xi_l \sum_{M=1, N=1}^{\infty} x^M y^N Q_{NM} \Gamma_M \Gamma_N M N, \quad (4)$$

by the following equation

$$W(x, y) = W(x)W(y)(\exp Q(x, y) - 1). \quad (5)$$

Expanding equation (5) one can compute cumulant correlators Q_{NM} from factorial moments W_{NM} .

$$\begin{aligned} Q_{12} 2\Gamma_1 \Gamma_2 \xi_r &= w_{12}/2 - \xi_r \\ Q_{13} 3\Gamma_1 \Gamma_3 \xi_r &= w_{13}/6 - w_{12}/2 - w_{20}/2 + \xi_r \\ Q_{22} \Gamma_2^2 4\xi_r &= w_{22}/4 - w_{12} + \xi_r - \xi_r^2/2 \end{aligned} \quad (6)$$

As it is clear from equations (6), cumulant correlators are determined by two different length scales, length scale corresponding to ξ_s and scale corresponding to ξ_r . We use the terms quasi-linear and nonlinear depending upon values of ξ_s .

2.1 Nonlinear Regime

The extreme nonlinear stage of gravitational clustering is believed to be well described by a power law solution for correlation function $\xi_2 = r^{-\gamma}$, where γ can be expressed as a function of initial power spectrum (Davis & Peebles 1977, Balian & Schaeffer 1989. All higher order correlations exhibit a self similar scaling in strong clustering regime

$$\xi_N(\lambda \mathbf{r}_1, \dots, \lambda \mathbf{r}_N) = \lambda^{-\gamma(N-1)} \xi_N(\mathbf{r}_1, \dots, \mathbf{r}_N). \quad (7)$$

More explicit functional forms for N -point correlations are constructed by summing over products of $N-1$ two-point correlation functions corresponding to different topologies, each of which representing a tree graph spanning N -points with amplitudes $T_{n,\alpha}$

$$\xi_N(\mathbf{r}_1, \dots, \mathbf{r}_N) = \sum_{\alpha, N\text{-trees}} T_{N,\alpha} \sum_{\text{labelings}} \prod_{\text{edges}}^{(N-1)} \xi_{(r_i, r_j)}. \quad (8)$$

Tree graphs spanning three points can have only one topology. The amplitude associated with this graph Q_3 contributes through three different configurations of these points, so that cumulant correlators to have following form:

$$\langle \delta(\mathbf{x}_1)^2 \delta(\mathbf{x}_2) \rangle = 2Q_{12} \xi_s \xi_r = Q_3 (2\xi_s \xi_r + \xi_r^2). \quad (9)$$

Higher order cumulants get contributions from different types of tree diagrams. At fourth order trees connecting four points have two different topologies, known as the snake (with its amplitude denoted by R_a) and the star topology (corresponding amplitude denoted conventionally by R_b). Using this notation we can write

$$\langle \delta_1(\mathbf{x}_1)^3 \delta_2(\mathbf{x}_2) \rangle = 9Q_{13} \xi_r \xi_s^2 = 6\xi_r \xi_s^2 R_a + 3\xi_r \xi_s^2 R_b + 6\xi_r^2 \xi_s R_a + \xi_r^3 R_b \quad (10)$$

$$\langle \delta(\mathbf{x}_1)^2 \delta(\mathbf{x}_2)^2 \rangle = 4Q_{22} \xi_r \xi_s^2 = 4\xi_r \xi_s^2 R_a + 4\xi_r^2 \xi_s R_b + 4\xi_r^2 \xi_s R_a + 4\xi_r^3 R_b. \quad (11)$$

These simultaneous equations are linear in R_a and R_b and can be solved once Q_{22} and Q_{13} are determined. When $\xi_r \ll 1$ which will be the case when two cells are far away, one can define linear cumulant correlators (linear in ξ_r) by considering only terms linear in ξ_r . The linear solution to equation (11) are $R_a = Q_{22}$ and $R_b = 3Q_{13} - 2Q_{22}$. In such a linear accuracy one can show that

$$Q_{NM} \approx Q_{N+M} \quad (12)$$

Although amplitudes of tree terms with different topologies can be estimated by cumulant correlators, the situation becomes more complicated at higher order as number of degenerate correlators become less than number of topologies, making the system indeterministic. Other interesting questions regarding scaling of generating functions $Q(x, y)$ and related question about the nature of Q_{NM} in the highly nonlinear regime can be addressed when bigger N -body simulations become available.

2.2 Quasi-linear Regime

In quasi-linear regime when ξ_s is smaller than unity it is possible to expand $\delta = \delta^{(1)} + \delta^{(2)} + \delta^{(3)} \dots$ where perturbation expansion is valid as long as the series is convergent. Using perturbative calculation of two point quantities it was possible for Bernardeau (1996) to express C_{pq} at lowest order. Perturbative terms contributing to the expansion of $\langle \delta^p(\mathbf{x}_1) \delta^q(\mathbf{x}_2) \rangle$ can be written as

$$\langle \delta^p(\mathbf{x}_1)\delta^q(\mathbf{x}_2) \rangle \approx \sum_{\text{decompositions}} \left\langle \prod_{i=1}^p \delta^{(p_i)}(\mathbf{x}_1) \prod_{j=1}^q \delta^{(q_j)}(\mathbf{x}_2) \right\rangle \quad (13)$$

where sum is taken over all possible decompositions and p_i and q_i satisfies

$$\sum_{i=1}^p p_i + \sum_{j=1}^q q_j = 2(p+q) - 2. \quad (14)$$

In lowest order in perturbation theory it is possible to write (Bernardeau 1996),

$$\langle \delta^p(\mathbf{x}_1)\delta^q(\mathbf{x}_2) \rangle_c = C_{pq} \langle \delta^2(x) \rangle^{p+q-2} \langle \delta(x_1)\delta(x_2) \rangle = C_{pq} \xi_s^{p+q-2} \xi_r. \quad (15)$$

Using method of generating function it was shown that C_{pq} can be decomposed into following relation (Bernardeau, 1996),

$$C_{pq} = C_{p1}C_{q1}. \quad (16)$$

In 3D the lowest order C_{pq} can be expressed in terms of spectral index n ,

$$C_{21} = 68/21 - 1/3(n+3) \quad (17)$$

$$C_{31} = 11710/441 - 61/7(n+3) + 2/3(n+3)^2. \quad (18)$$

It should be noted that such factorization is possible only in case of tree-level diagrams also calculations were done using large separation limit. Given the whole hierarchy of C_{NM} it is possible to compute bias associated with gravitational clustering in the quasi-linear regime (Bernardeau 1996).

2.3 Connecting different regimes: Extended Perturbation Theory

Tree level perturbation theory can predict S_N parameters for top-hat smoothing, it was used (as out lined above) to compute cumulant correlators $Q_{N,M}$ to arbitrary order in large separation limit. The expressions derived for cumulants depends on index of initial power spectrum. However it was later realized that the same quasi-linear expressions can describe evolution of S_N parameters from quasi-linear regime to the nonlinear regime by allowing spectral index n to vary with scale (Colombi et al. 1996b). It is interesting that whole hierarchy of S_N can be described by such a variation of effective spectral index n_{eff} (unfortunately no straight forward relation exists between true nonlinear power spectra and n_{eff}). An extension of perturbation theory to the non-perturbative regime was considered by Szapudi & Szalay (1997) for cumulant correlators $Q_{N,M}$. Tree level perturbation theory as mentioned before predicts $C_{pq} = C_{p1}C_{q1}$. Using same logic as extended perturbation theory one can expect such a relation to hold even for small cell sizes at large distances although separately each of these term may vary significantly.

3. Simulations and Data Analysis

The simulations used here are numerical models for the gravitational clustering of collisionless particles in an expanding background. We study evolution of initial Gaussian perturbations in $\Omega = 1$ universe. All the 2D simulations are done with a particle-mesh (PM) code with 512^2 particles with an equal number of grid points and in 3D 128^3 particles with 128^3 grid points The code has at least twice the dynamical resolution of any other PM code with which it has been compared. The 2D simulations are described in detail in Beacom et. al (1991), with a video of the evolution in Kauffmann and Melott (1992). The 3D simulations are described in Melott and Shandarin (1993). Both sets, which consist of multiple realizations (different random seeds) for a variety of power spectra, have been widely used for comparative studies of various statistical methods and dynamical approximations.

Fig. 1.— Lower panel displays factorial moment correlators w_{kl} as a function of separation r in 2D in units of grid scale. Degenerate parallel lines correspond to increasing values of $N + M$ from 2 to 6. Left panels display results for scale free spectra with power law index $n = -2$, middle panel for $n = 0$ and right panel $n = 2$ in two dimension. Middle and upper panels plot cumulant correlators of different orders. Dashed curves in middle panels represent $Q_{N1}Q_{M1}$ for different values of N and M , closest solid curves represent Q_{NM} for same values of N and M . According to predictions from extended perturbation theory they should overlap $Q_{NM} = Q_{N1}Q_{M1}$. Top most panels compare predictions of hierarchal ansatz $Q_{NM} = Q_{N+M}$. Adjacent curves correspond to different N and M with same $N + M$. Error bars were calculated by finding scatter in results with different realization of same initial power spectra.

Fig. 2.— Same as Figure - 1 but results from only one realization are plotted to show level of agreement with theoretical predictions in individual realizations.

In this paper we analyze a subset of the simulations with featureless power-law initial spectra of the general form,

$$\begin{aligned} P(k) &\propto k^n \text{ for } k \leq k_c, & (19) \\ &= 0 \text{ for } k > k_c. & (20) \end{aligned}$$

We have analyzed power-law models with $n = 2, 0, -2$ in 2D and $n = 1, 0, -1, -2$ in 3D with a cutoff in each case at the Nyquist wave number: $k_c = 256 k_f$ for 2D and $k_c = 64 k_f$ for 3D where $k_f = 2\pi/L_{\text{box}}$ is the fundamental mode associated with the box size.

We choose $\sigma(k_{\text{NL}})$, the epoch when the scale $2\pi/k_{\text{NL}}$ is going nonlinear as a measure of time.

$$\sigma(k_{\text{NL}}) = \left(\frac{\int_{k_f}^{k_{\text{Ny}}} P(k) k \, dk}{\int_{k_f}^{k_{\text{NL}}} P(k) k \, dk} \right)^{\frac{1}{2}} \quad (21)$$

The first scale to go nonlinear is the one corresponding to the Nyquist wave number. This happens, by definition, when the variance σ is unity. Of course as σ increases successive larger scales enter in the nonlinear regime. The simulations were stopped at $\lambda_{\text{NL}} = 2l_{\text{grid}}, 4l_{\text{grid}}, 8l_{\text{grid}}, \dots, L_{\text{box}}/2$. In our study in 2D we took the epoch when $L_{\text{box}}/16$ for analysis of $n = -2$ spectrum and for $n = 0$ and 2 we studied the epoch when $L_{\text{box}}/8$ is going nonlinear. In 3D we had less dynamic range so choose the epoch when $L_{\text{box}}/4$ for analysis of $n = -2$ spectrum and for $n = -1, 0,$ and 1 we studied the epoch when $L_{\text{box}}/2$ is going nonlinear. The separation r that we study is much less compared to the length scale going nonlinear so it is unlikely that our results will be affected much by boundary conditions.

The growth rate of various modes in the linear regime were studied by Melott et al. (1988) for this PM code. The results at $\lambda = 3l_{\text{grid}}$ are equivalent to the ones obtained by a typical PM code at $\lambda = 8l_{\text{grid}}$, due to the staggered mesh scheme. So we expect that our code performs well at the wavelength associated with four cells and since the collapse of $4l_{\text{grid}}$ -size perturbations will give rise to condensations of diameter $2l_{\text{grid}}$ or less, the smallest cell size that can be safely resolved is $2l_{\text{grid}}$.

Computations of count probability distribution function (CPDF) $P_l(n)$ and two-point count probability distribution $P_{l,r}(n, m)$ were done by laying down a grid of mesh spacing l and counting occupation number in each cell to compute the probability of finding n objects in cell size l and also the joint probability of finding n and m objects in two cells separated by a distance r . Statistics were improved by perturbing the grid in each orthogonal direction and keeping the mesh undistorted while repeating the counting process. Both in two and three dimensions we considered only cells of size l_{grid} . While this particular choice of cell size is open to question, we will show that our results match remarkably well with our earlier studies done using bigger cell sizes. With this cell size we could reach probabilities as few times 10^{-6} in 2D and 3D. Computations of factorial moments and factorial moment correlators were done using computed values of $P_l(n)$ and $P_{l,r}(n, m)$. Computed values of ξ_2 for cells used were found to be 8.98, 27.87, 60.39 in 2D for spectral index $-2, 0,$ and 2 respectively. In 3D these values were found to be 25.46, 88, 125.5, and 171 respectively.

Different spurious effects such as shot noise and finite volume corrections are important while computing count probability distribution functions. For small cell sizes Poisson noise starts dominating, whereas larger cell sizes are dominated by finite volume corrections. We find w_{kl} parameters to be dominated by shot noise with increasing separation of cells, this effects starts to be severe with higher order cumulants. This effect starts dominating even for small separation for spectra with less power on larger scales. Using large cells produces effect similar to smoothing the density field and hence reducing the effective correlation length scale between them. These two dominant effects reduce the range of separation which can be probed for studying cumulant correlators. Finite volume corrections are more difficult to quantify. Methods based on scaling of count in cell statistics were shown to be effective in correcting finite volume effects (Munshi et al. 1997), similar arguments can be used to develop corrections for cumulant correlators. The validity of such a method depends on correctness of the scaling model, which we test in this paper. Developments of methods to correct Q_{NM} for finite volume effect are left for future work.

Computed w_{kl} for 2D simulations are plotted in Figure - 1 as a function of cell separation r . Corresponding results for 3D are presented in Figure - 5. Parallel degenerate lines correspond to different values of $N +$

Fig. 3.— Lower order hierarchal amplitudes Q_3 , R_a , R_b calculated from the fully nonlinear cumulative correlators in 2D are plotted against separation r measured in grid units. Solid curve represent estimates of Q_3 lower and upper dashed lines represent amplitudes of fourth order snake and star graphs R_a and R_b respectively. Open triangles and square correspond measurement of Q_3 and Q_4 respectively from factorial moments of counts in cell statistics after finite volume corrections were taken into account (from Munshi et al. 1997). Filled triangles and squares are measurements of same quantities using cumulant correlators without finite volume correction.

Fig. 4.— Each panel displays factorial moment correlators w_{kl} as a function of separation r in unit of grid scale for different initial scale-free power law spectra in 3D. Scatter in each plot is computed from scatter in four different realizations of same power spectra.

Fig. 5.— Nonlinear cumulant correlators is plotted against separation r in 3D as measured in units of grid scale. Uppermost curve correspond to Q_{31} , lowest curve to Q_{22} and the dashed one to Q_{21}^2 . Solid and dashed straight lines correspond to predictions for Q_{31} , and Q_{21}^2 from perturbations theory at large separation.

Fig. 6.— Hierarchal amplitudes Q_3 , R_a , R_b calculated from the nonlinear cumulative correlators in 3D are plotted against separation r measured in grid units. Solid curve represent estimates of Q_3 lower and upper dashed lines represent amplitudes of fourth order snake and star graphs R_a and R_b respectively. Open triangles and square correspond to measurement of Q_3 and Q_4 respectively from factorial moments of counts in cell statistics after finite volume corrections were taken into account (from Munshi et al. 1997). Filled triangles and squares are measurements of same quantities using cumulant correlators without finite volume correction.

M increasing from bottom to top in each panel. Middle and top panels show variation of Q_{NM} with r . Middle panels test the validity of extended perturbation theory. Dashed lines correspond to $Q_{N1}Q_{M1}$ while neighboring solid lines represent Q_{NM} for same values of N and M . Error bars are computed by estimating the scatter in results from four different realization of each spectra. It is interesting to note that while Q_{NM} shows an increasing trend with increasing $N + M$ for spectra with large scale power $n = -2$ in 2D, the trend is reversed for $n = 0$ and 2 . The results presented in 2D are for $N + M = 4, 5$ and 6 respectively. In 3D meaningful computation of $Q_{N,M}$ were possible only for $N + M < 4$. We find that computed values of Q_{NM} are more stable towards fluctuation at large separation if one of the indices of cumulant correlators is larger than the other (e.g. w_{31} is more stable at larger separation as compared to w_{22}). Close associations of dashed curves with solid curves proves the validity of extended perturbation theory. It is also easy to notice that agreement is better in case of 2D compared to 3D. Larger simulation size might be a possible explanation for such an effect. Given that we restrict our result to highly nonlinear regime, it is interesting to note that computed values of C_{NM} are not completely different from predictions of perturbation theory at large separation. In Figure - 5, dashed and solid straight lines are predicted values of Q_{21}^2 and Q_{31} from equation (17) and equation (18). Top panels in Figure - 1 and Figure - 5 tests the validity of equation (12) in 2D and 3D respectively. Nearest neighbor curves correspond to different values of N and M which produces same $N + M$. Agreement in this case is similar to that of extended perturbation theory.

Using cumulant correlators it is possible to compute amplitudes of different tree topologies contributing to four and five point correlation functions. We have computed amplitudes Q , R_a and R_b . Figure - 3 shows that these amplitudes are almost constant in 2D in the highly nonlinear regime. In 3D Figure - 6 shows large fluctuations in computed values of R_b although in general they are fairly constant within the limited range of nonlinearity studied by us. Open triangles and squares denote measured values of Q_3 and Q_4 using factorial moments of CPDF. On the other hand solid triangles and squares denotes measured values of Q_3 and Q_4 from cumulant correlators. Q_4 was calculated by using the relation $16Q_4 = 12R_a + 4R_b$, from computed average values of R_a and R_b . The remarkable agreement of both the methods increases confidence in results based on cumulant correlators. It is also to be noted that whereas computation of one point cumulants were done by taking volume corrections into account, such effects were neglected in the computation of cumulant correlators. Our results show that Q_4 is much closer to R_b which might indicate that star topologies in general dominate over snake topologies. However, more systematic studies are necessary which will incorporate finite volume effects and have more dynamic range than this study.

6. Discussion

Measurements of cumulant correlators and lower order one point cumulants have already been done for Lick catalog, SDSS and the APM survey. Analyzing cumulant correlators in the APM survey, Szapudi & Szalay (1997) demonstrated the validity of the hierarchal ansatz to unprecedented accuracy. They found $Q_3 = 1.15$, $R_a = 5.3$ and $R_b = 1.15$. These results were also shown to be in good agreement with computation of one point cumulants based on factorial moments $Q_3 = 1.7$ and $Q_4 = 4.17$. Measurements from SDSS give $Q_3 = 1.16$ and $Q_4 = 2.96$. It was suggested that slightly low value of Q_4 from SDSS was lack of nonlinear corrections in their computations. Other measurements from APM produces $Q_3 = 1.6$ Szapudi et al. (1996) and $Q_3 = 1.7$ by Gaztanaga (1994). The values of fourth order cumulants found by these authors were $Q_4 = 3.2$ and $Q_4 = 3.7$ respectively.

Use of methods based on cumulant correlators by Szapudi and Szalay has produced lower values for R_b compared to R_a . In our simulations both in 2D and 3D we find that relative position of these two amplitudes depend on initial power spectra. In all cases R_b was found to be either equal to or greater than R_a , although the separation was found to decrease with increasing n . For power spectra such as $n = 1$ in 3D and $n = 2$ in 2D which have more power at smaller scales these two quantities are found to almost coincide with each other. Although this is in disagreement with findings of Szapudi and Szalay (1997), our results seems to be closer to that of by Fry & Peebles (1978) who found $R_a = 2.5 \pm 0.6$ and $R_b = 4.3 \pm 1.2$ from their analysis of Lick catalog. At any rate, they are analyzing data in projection, and we a simulation with full information. We do not know to what extent projection and the possible inclusion of non-gravitational physics may influence the results.

There have been several attempts to solve BBGKY equations in the highly nonlinear regime, although no general solution exists so far. Attempts were made to solve these equations by assuming specific separable hierarchical forms for higher order correlations in phase space. Fry (1982) derived $Q_{N,\alpha} = Q_N = (4Q/N)^{N-2}N/(N-2)$, in particular this model predicts $R_a = R_b = Q_4 = 2Q^2/3$. Hamilton (1988) redoing the analysis found only snake topologies to contribute in higher order correlations while all non-snake contributions vanish identically which gives $Q_N = (Q/N)^{N-2}N!/2$. For lower order amplitudes this predicts $R_a = Q^2$, $R_b = 0$ and $Q_4 = 3Q^2/4$. The ansatz used by Bernardeau and Schaeffer (1992) predicts $R_a = Q_3^2$. While all these efforts to solve BBGKY equations provide useful insight into complications arising due to the nonlinear nature of the problem, it is clear from our study that cumulant correlators are a very useful tool in comparing such predictions with computer simulations. The general agreement of 2D and 3D results reinforces the many other results which have shown that 2D may be a useful tool to extend the dynamic range for exploration of statistics in cosmology.

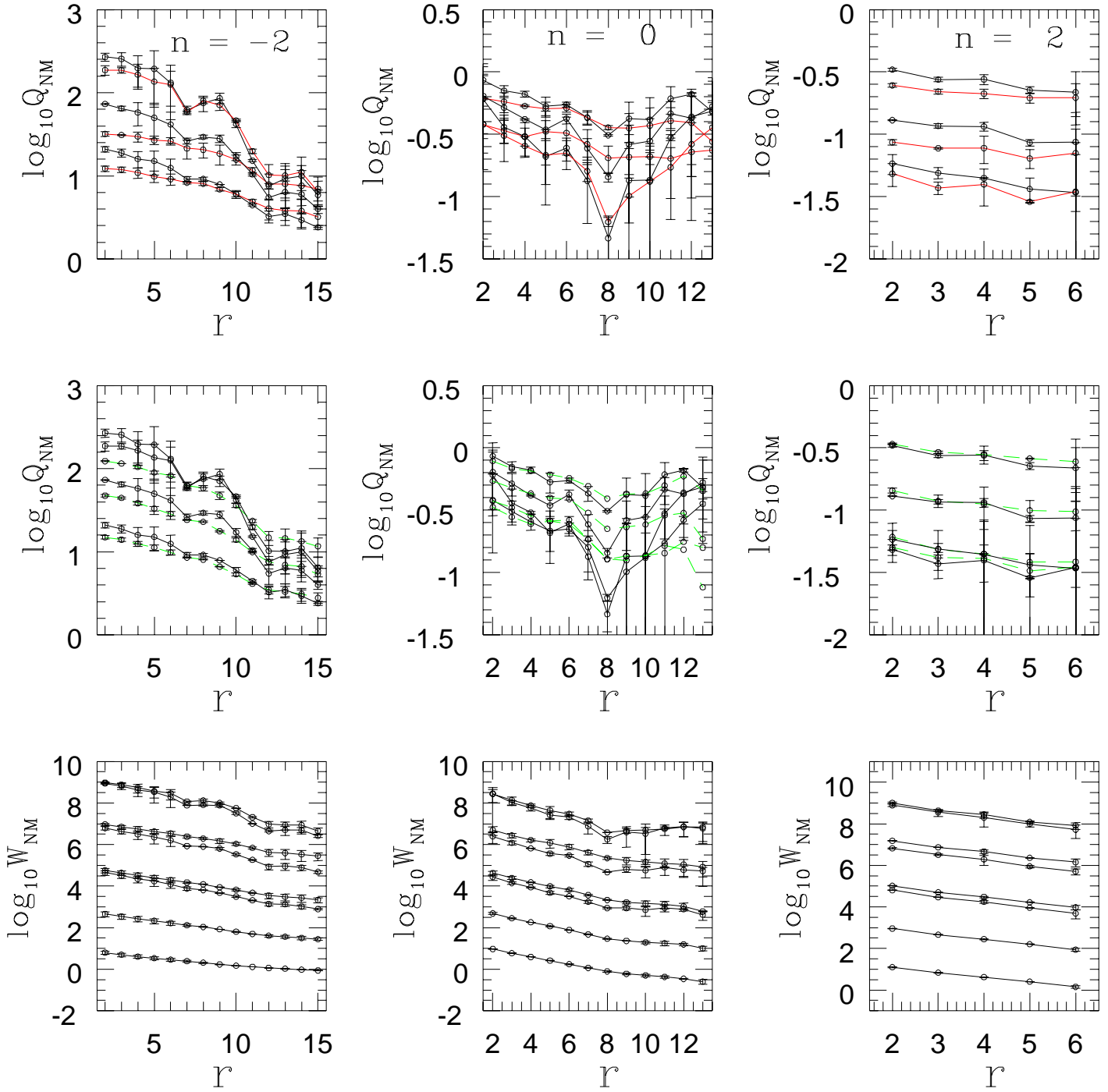
Acknowledgements: D.M. acknowledges support from PPARC under the QMW Astronomy Rolling Grant GR/K94133. A.L.M. wishes to acknowledge the National Center for Supercomputing Applications for support to perform the ensemble of simulations, and the financial support of the NSF EPSCoR program.

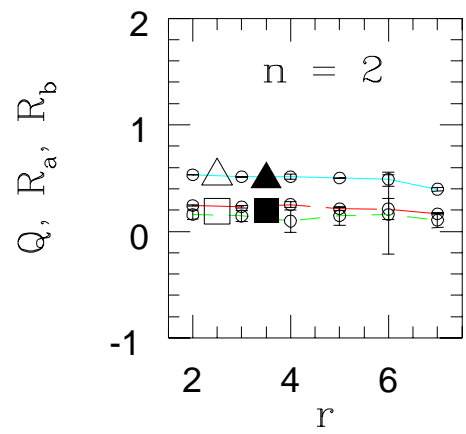
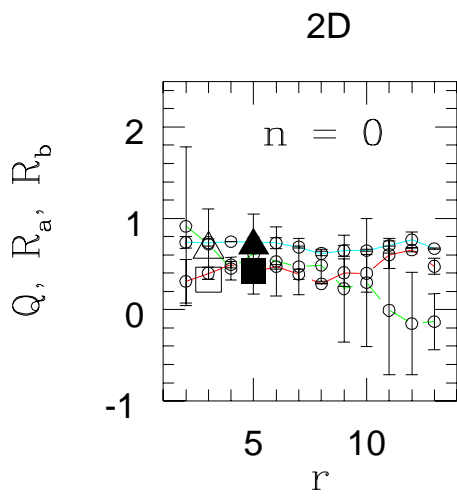
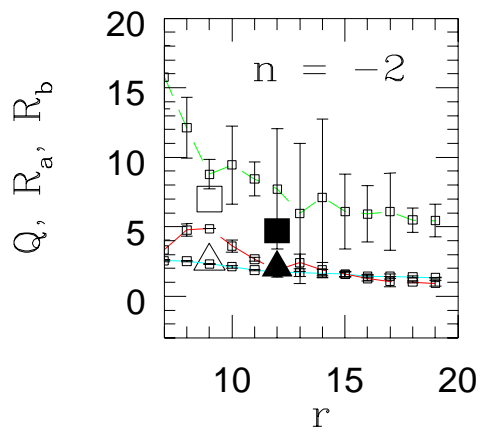
REFERENCES

- Balian, R., & Schaeffer, R. 1989, *A & A*, **220**, 1
- Beacom, J.F., Dominik, K.G., Melott, A.L., Perkins, S.P., & Shandarin, S.F. 1991, *ApJ*, **372**, 351
- Bernardeau, F. 1992 *ApJ*, **392**, 1
- Bernardeau, F. 1994b, *ApJ*, **433**, 1
- Bernardeau, F. 1995, *A&A*, **301**, 309
- Bernardeau, F. & Schaeffer, R. 1992, *A&A*, **255**, 1
- Boschan, P., Szapudi, I., & Szalay, A. 1994, *ApJS*, 93, 65
- Baugh, C.M., & Gaztanaga, E., 1996, *MNRAS*, 280, L37
- Bouchet, F.R., Strauss, M.A., Davis, M., Fisher, K.B., Yahil, A., & Huchra, J.P., 1993, *ApJ*, 417
- Colombi, S., Bouchet, F.R., & Hernquist, L., 1996a, *ApJ*, 465, 14
- Colombi, S., Bouchet, F.R., & Schaeffer, R., 1995, *ApJS*, 96, 401
- Colombi, S., Bernardeau, F., Bouchet, F.R., & Hernquist, L. 1996b (astro-ph/9610253)
- Fry, J.N., & Gaztanaga, E., 1993, *ApJ*, 413, 447
- Fry, J.N., & Peebles, P.J.E., 1978, *ApJ*, 221, 19
- Gaztanaga, E. 1992, *ApJ*, 319, L17
- Gaztanaga, E., 1994, *MNRAS*, 268, 913
- Gaztanaga, E., & Frieman, J.A., 1994, *ApJ*, 437, L13
- Hamilton, A.J.S., 1988, *ApJ*, 332, 67
- Kauffmann, G.A.M., and Melott, A.L. 1992, *ApJ* 393, 415
- Juszkiewicz, R., Bouchet, F.R., & Colombi, S. 1993, *ApJ*, 412, L9
- Meiksin, A., Szapudi, I., & Szalay, A., 1992, *ApJ*, 394, 87

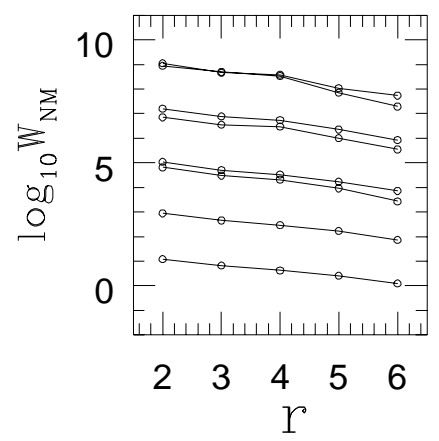
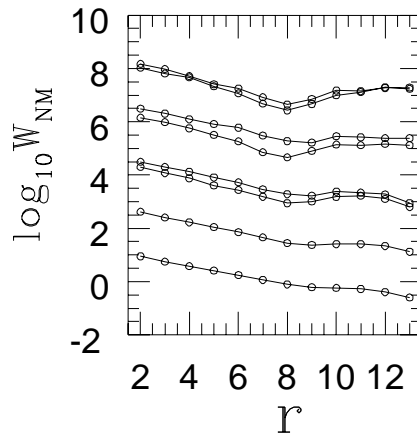
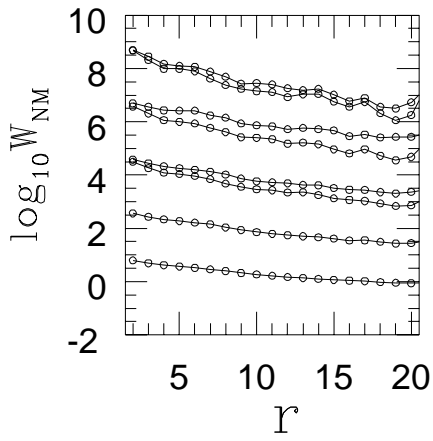
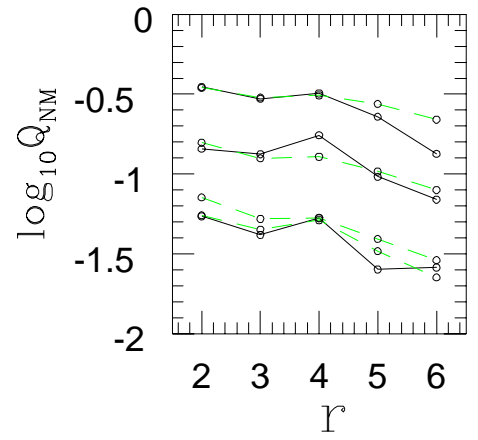
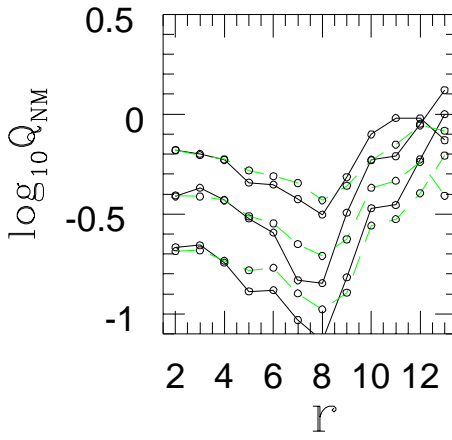
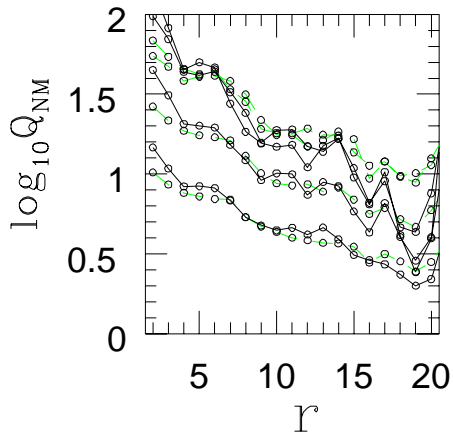
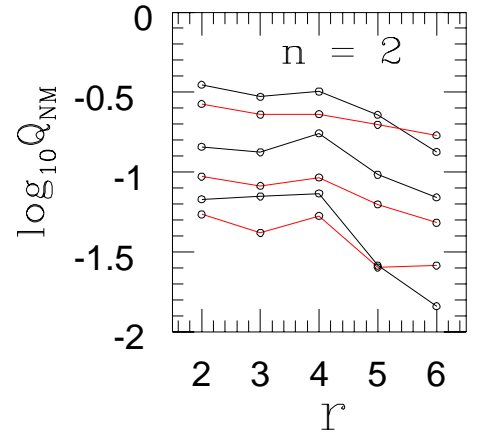
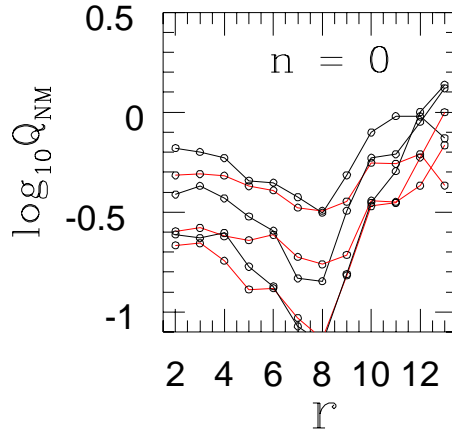
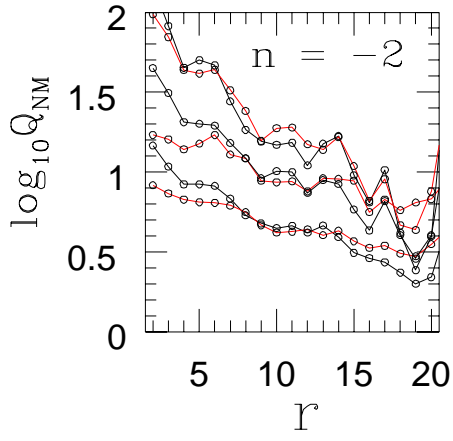
Melott, A.L., and Shandarin, S.F. 1993 ApJ 410, 469
Melott, A.L., Weinberg, D.H., and Gott, J.R. 1988 ApJ 328, 50
Munshi, D., Sahni, V., Starobinsky, A. A. 1994, ApJ, **436** 517
Munshi, D., Bernardeau, F., Melott, A. L., & Schaeffer, R. 1997, (astro-ph/9707009)
Peebles, P.J.E., 1980, The Large Scale Structure of the Universe (Princeton University Press)
Scoccimarro, R. & Frieman, J. 1996a, ApJS, **105**, 37
Scoccimarro, R. & Frieman, J. 1996b, ApJ, **473**, 620
Szapudi, I. & Colombi, S., 1996, ApJ, 470, 131
Szapudi, I., Dalton, G., Efstathiou, G.P., & Szalay, A., 1995, ApJ, 444,520
Szapudi, I. & Szalay, A. 1993, 1pJ, 408, 43
Szapudi, I., Szalay, A., & Boschan, P., 1992, ApJ, 390, 350

2D

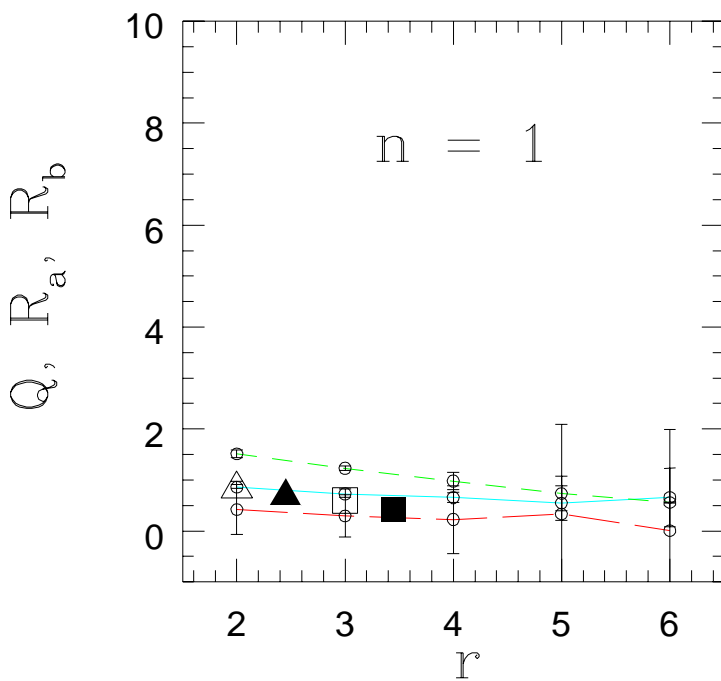
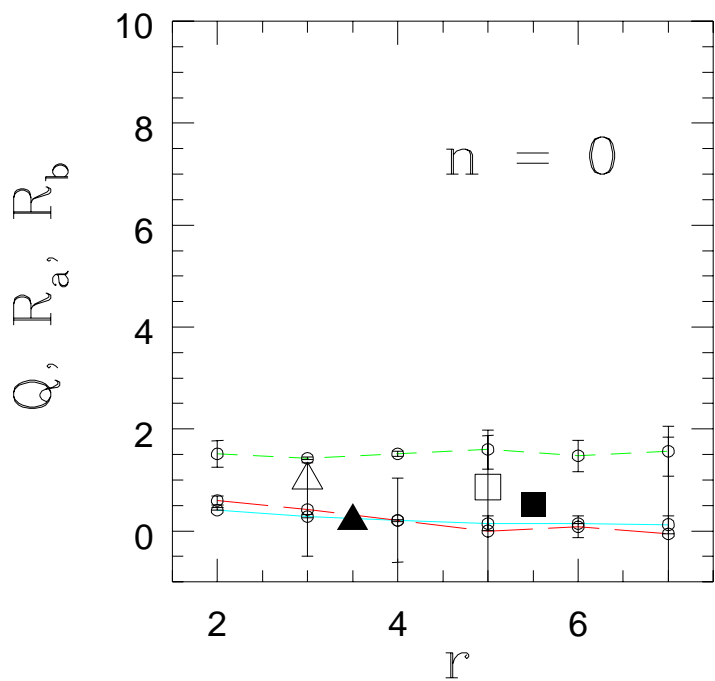
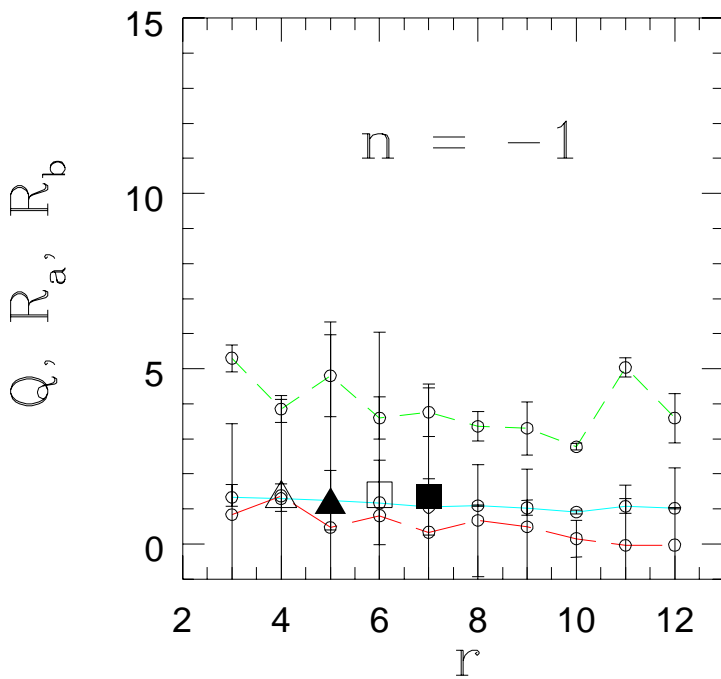
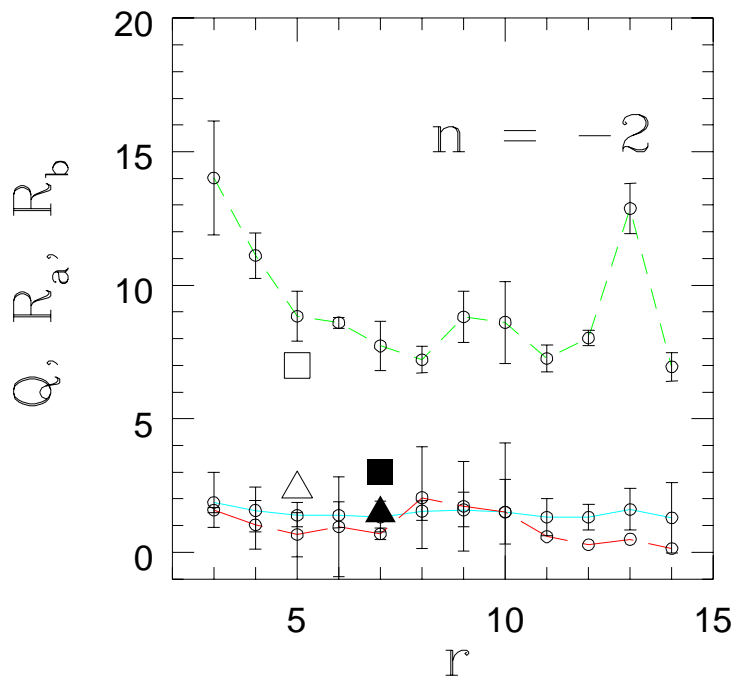




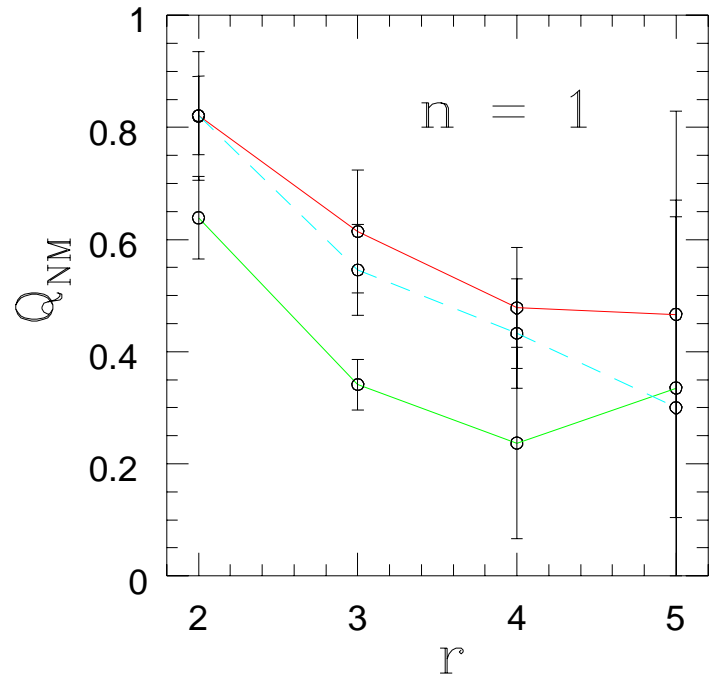
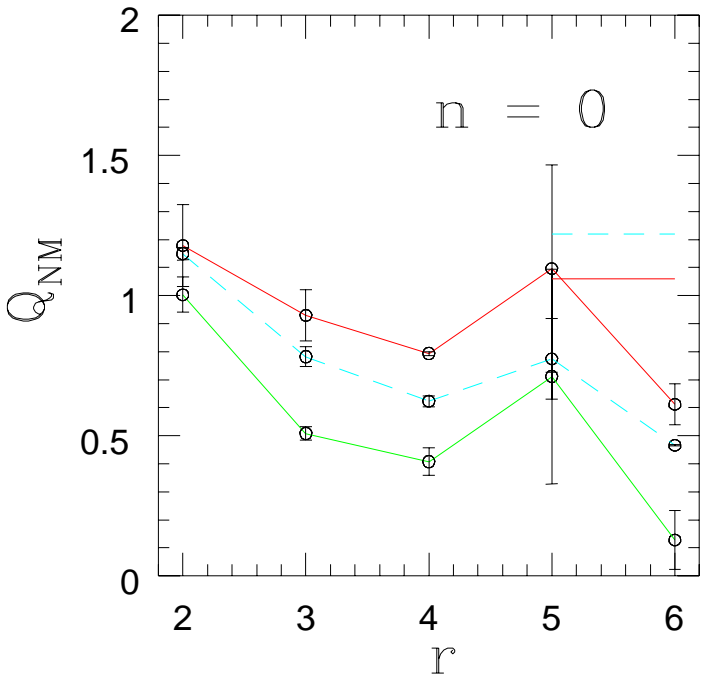
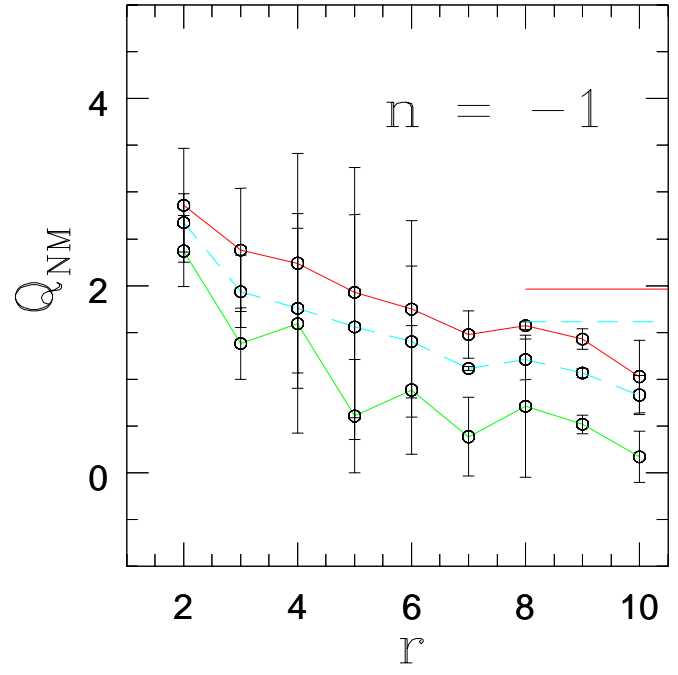
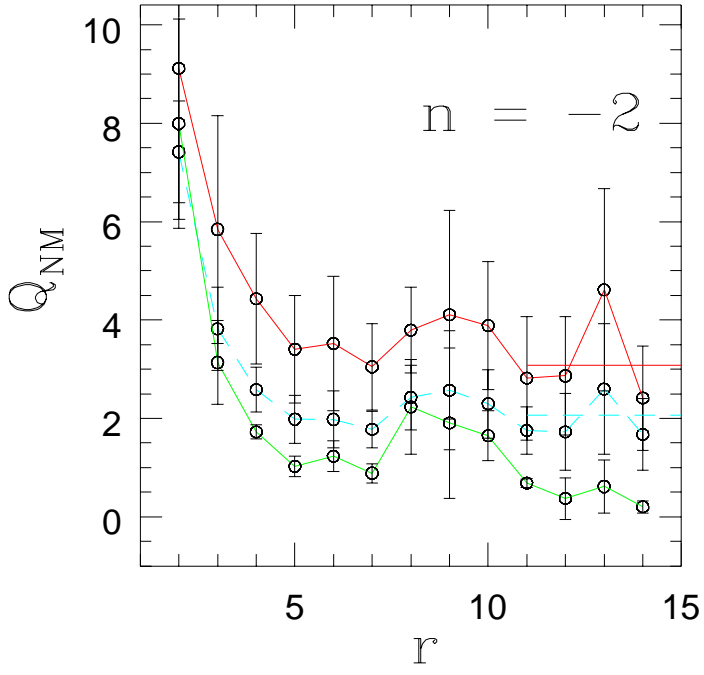
2D



3D



3D



3D

